The Martian oxygen red line airglow: observations with NOMAD/UVIS and modeling

J.-C. Gérard, LPAP, *STAR Institute, Université de Liège, Belgium (jc.gerard@uliege.be)*, ***L. Soret,*** LPAP, *STAR Institute, Université de Liège, Belgium, L. Gkouvelis,* **L. Gkouvelis**, *NASA Ames Research Center, CA, United States*, **S. Aoki**, *University of Tokyo, Japan, and the* ***NOMAD/UVIS team***

Detection of visible emissions. The Ultraviolet and Visible channel (UVIS) of the NOMAD instrument (Vandaele et al., 2018; Patel et al., 2017) on board the EXOMARS Trace Gas Orbiter (TGO) has been observing the dayside limb of the planet since April 2019. For this purpose, the TGO spacecraft in moved in such a way that the nadir channel of the instrument is oriented to the sunlit limb away from the Sun's direction. The instrument is occasionally operated to collect spectra in the inertial limb mode where the instrument points at the dayside limb in a fixed orientation (López-Valverde et al., 2018). By virtue of the spacecraft motion along its orbit, the line of sight scans through the atmosphere down to a predetermined altitude of the tangent point and detects ultraviolet and visible dayglow emissions. In this inertial tracking mode, only two altitude scans through the atmosphere (one ingress and one egress) are collected during one TGO orbit. In contrast, in the limb tracking mode, the UVIS boresight is constrained to remain in the vicinity of a preset tangent altitude while the tangent point of the line of sight moves in latitude under the effect of the orbital motion. Actually, the tangent altitude usually stabilizes within ~20 km during the course of an observation sequence. Different fixed altitudes have been selected to optimize the observing time near the peak altitude. Only spectra collected when the solar zenith angle at the tangent point was less than 70° are used in this study (Soret et al., 2022).

The 630-nm emission is too weak to determine limb profiles based on spectra collected during a single TGO orbit. Therefore, we have averaged the observed limb distribution of the global dataset and determined the intensity inside 20 km wide altitude bins.

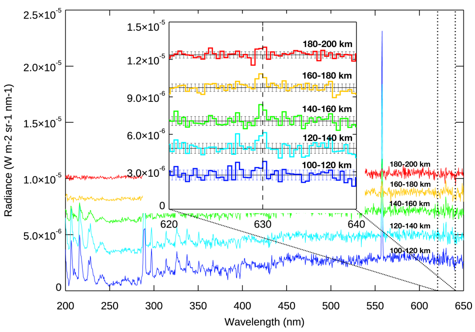

Figure 1: UVIS mean limb spectra averaged in 20-km altitude bins. The insert is a zoom on the 620–640 nm region. The dotted line indicates the 630 nm wavelength position (Gérard et al., 2021).

The red line feature is observed in all altitude bins, confirming the reality of its detection. It shows a peak much broader than other emissions such as the CO_2^+ UV doublet or the [OI] green line. A peak intensity of ~4.8 kR is observed in the 120-140 km bin of tangent altitude. The large values of the uncertainty compared to the mean intensity are a consequence of both the low observed brightness and the true variability largely due to the combination of observations at different latitudes, solar longitudes and solar zenith angles.

The red line doublet. The O ($^1D \rightarrow {}^3P$) transition giving rise to the red emission is a doublet with a second, weaker, component at 636.4 nm. This second component is a factor of 3 to 3.1 weaker than the one at 630 nm (Fischer and Tachiev, 2004; Sharpee and Slanger, 2006). Although it was not initially detected, accumulation of spectra now makes it possible to observe the second doublet component (Figure 2). We observe a I(630 nm)/I(636.4 nm) intensity ratio in full agreement with the expected ratio, definitely confirming the identification.

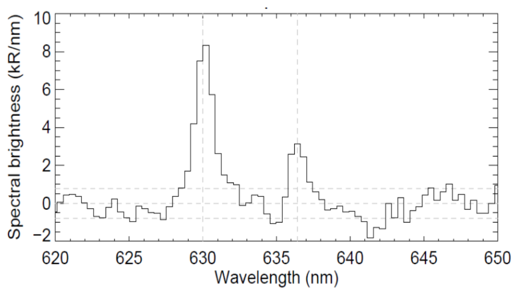

Figure 2: average UVIS-IUVS spectrum showing the red line doublet. The horizontal dashed lines show the 0 signal level and ±1σ noise level (Soret et al., 2022).

Model.

We use the Photochemical Airglow Mars (PAM) model (Gkouvelis et al., 2018; Gérard et al., 2021; Soret et al., 2022) to calculate the production, loss and brightness of the red line dayglow. Figure 3 shows the altitude distribution of the O(^{1}D) main sources. The production processes are similar to O(^{1}S). However, the O(^{1}D) density peaks significantly higher than O(^{1}S) because its radiative lifetime is more than two orders of magnitude longer and collisional quenching plays a major role. Unlike O(^{1}S)

(Gérard et al., 2020) the simulated limb intensity shows a single peak near 140 km, in agreement with the observations.

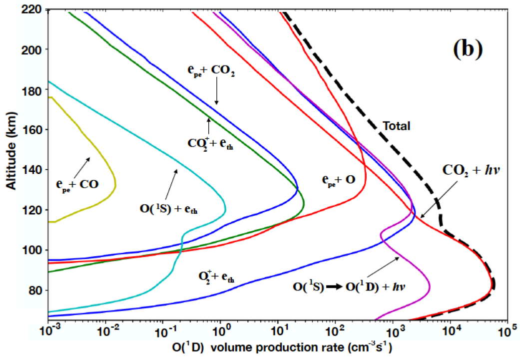

Figure 3: volume production rate of $O(^1D)$ atoms in the dayglow. The individual contributions are indicated in different colors and the total production rate corresponds to the black dashed line.

We also present the observed seasonal variations of the 630-nm airglow and compare them with other dayglow emissions, including the OI 557.7 nm emission.

References

Fischer, C. F., & Tachiev, G. (2004). Atomic Data and Nuclear Data Tables, 87(1), 1-184.

Gérard, J. C., et al. (2020). Nature Astronomy, 4(11), 1049-1052.

Gérard, J.C. et al. (2021). Geophysical Research Letters, 48(8).

Gkouvelis, L. et al., (2018). Journal of Geophysical Research: Planets, 123(12), 3119-3132.

López-Valverde, et al. (2018). Space Science Reviews, 214(1), 29.

Patel, M. R. (2017). Applied optics, 56(10), 2771-2782.

Sharpee, B. D., & Slanger, T. G. (2006). The Journal of Physical Chemistry A, 110(21), 6707-6710.

Soret et al. (2022). Submitted for publication.

Vandaele, A. C. (2018). Planet. Space Sci 119, 233-249.